Real-time range finder based on phase- and modulation-amplitude-locked laser diode interferometry

Takamasa Suzuki, MEMBER SPIE
Tatsuo Iwana
Osami Sasaki, MEMBER SPIE
Niigata University
Faculty of Engineering
8050 Ikarashi 2
Niigata, 950-2181 Japan
E-mail: takamasa@eng.niigata-u.ac.jp

Abstract. An interferometric range finder that uses both phase-locked and modulation-amplitude-locked techniques in a sinusoidal phase-modulating interference signal is described. It allows us to perform unambiguous and real-time distance measurement. Also, external disturbance superimposed on the interference signal is eliminated by the feedback control. Our preliminary experiments indicate a measurement error of 17.7 μm rms.
[DOI: 10.1117/1.1799071]

Subject terms: interferometry; laser diode; phase lock; modulation-amplitude lock; sinusoidal phase modulation.

Paper 040142 received Mar. 17, 2004; revised manuscript received May 26, 2004; accepted for publication May 26, 2004.

1 Introduction

Conventional interferometers cannot detect a distance that is larger than a half wavelength. Many kinds of approaches have been proposed to overcome this problem. Some of the most common approaches are multiple-wavelength interferometries that use two or more wavelengths. Generally, as two-wavelength interferometers use two separate laser sources,[1,2] it is difficult to align the optical axes, and the setup is complicated. In such cases, the wavelength tunability of a laser diode (LD) is very useful, in that we can use different wavelengths with a single LD. For instance, quasi-two-wavelength interferometry (QTWI) that uses a single LD has been proposed.[3] We also proposed QTWI and demonstrated measurements of a step profile[4] and of absolute distance.[5] In these measurements, we used *phase-locked* (PL) LD interferometry,[6] a method capable of measuring phases through feedback control. Although the optical setup in these devices is simple, the measurement range and the accuracy are restricted because the phase term of the interference signal is sensitive to the change of the optical path difference (OPD) and because the phase detection is much affected by external disturbances, respectively.

On the other hand, compared with the phase, the modulation amplitude is less sensitive to changes in the OPD. Some approaches, as in double sinusoidal phase-modulating (DSPM) interferometers,[7,8] use this feature for distance measurement. In these interferometers, two different sinusoidal signals are used simultaneously to modulate the interference signal. The distance is measured from the modulation amplitude in the sinusoidal phase-modulating (SPM) interference signal by use of a frequency analysis. But it is difficult to implement the measurement in real time, because a lot of calculations are required in a computer.

In this paper, a real-time range finder based on both PL and *modulation-amplitude-locked* (MAL) techniques is described. We control not only the phase but also the modulation amplitude in the SPM interference signal by means of electronic feedback circuits. Measurement ambiguity caused by phase wrapping is thereby eliminated. Combined PL and MAL techniques allow us to stabilize the interference signal and achieve real-time signal processing.

2 Principle

2.1 *Sinusoidal Phase Modulation of the Interference Signal*

The configuration of our system is shown in Fig. 1. We used a Fizeau interferometer whose initial OPD is $2L$. It consists of a beamsplitter (BS2) as a reference and a mirror (M) as an object. The signal-processing unit (SPU) is composed of a LD modulator (LM), feedback controllers (FBC1,FBC2), and an amplitude detector (AMD). Both FBC1 and FBC2 are simultaneously used to perform PL and MAL controls for the interference signal, respectively. The fundamental sinusoidal signal

$$I_a(t) = a \cos \omega_c t \tag{1}$$

is fed into the SPU from the oscillator (OSC). The amplitude of $I_a(t)$ is controlled by FBC2, and the modulation current

$$I_m(t) = m \cos \omega_c t \tag{2}$$

is generated so as to achieve MAL control. Thus the SPM interference signal

$$S(t) = S_{\mathrm{dc}} + S_0 \cos[Z \cos \omega_c t + \alpha(t)] \tag{3}$$

is obtained,[9] where

$$Z = 4\pi m \beta L / \lambda_0^2 \tag{4}$$

is the modulation amplitude, and

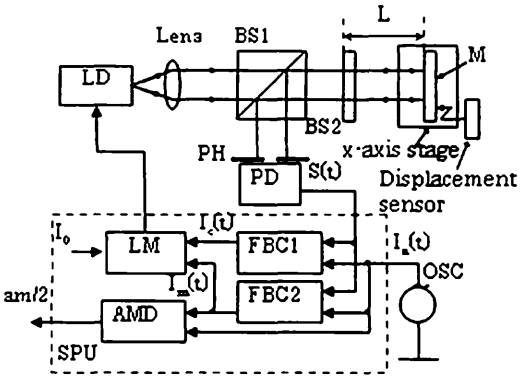

Fig. 1 Experimental setup: LD, laser diode; BS, beamsplitters; M, mirror; PH, pinhole; PD, photodiode; LM, laser modulator; FBC, feedback controllers; OSC, oscillator; AMD, amplitude detector.

$$\alpha(t)=4\pi L/\lambda_0 \tag{5}$$

is the phase, which depends on both the OPD and the wavelength used. The symbols S_0, β, and λ_0 represent the amplitude of the interference signal, the modulation efficiency, and the central wavelength of the LD, respectively. Finally, S_{dc1} is the dc component of the background intensity.

From the expansion of $S(t)$ expressed as

$$\begin{aligned}S(t)=S_{dc1}+S_0\cos\alpha(t)[J_0(Z)-2J_2(Z)\cos 2\omega_c t+\cdots]\\ -S_0\sin\alpha(t)[2J_1(Z)\cos\omega_c t-2J_3(Z)\cos 3\omega_c t\\ +\cdots],\end{aligned} \tag{6}$$

we can find that the second term of $S(t)$ contains another dc component,

$$S_{dc2}=S_0J_0(Z)\cos\alpha(t), \tag{7}$$

where $J_n(Z)$ is the n'th-order Bessel function. We eliminate S_{dc2} by use of the PL control as described in the next section.

2.2 *Phase-Locked and Modulation-Amplitude-Locked Controls*

In our system, both the PL and the MAL controls are implemented on the interference signal. The former is mainly used for eliminating S_{dc2}, and the latter is for the distance measurement. Here, we briefly explain them.

The block diagram of FBC1, which achieves PL control, is shown in Fig. 2. It consists of a frequency doubler (FRD), a multiplier, a lowpass filter (LPF), and a proportional-integral (PI) controller (PI1). The FRD doubles the frequency of $I_a(t)$. The output of the FRD is given by

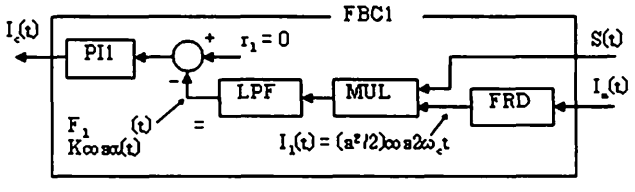

Fig. 2 Block diagram of FBC1: MUL, multiplier; LPF, lowpass filter; FRD, frequency doubler; PI1, proportional-integral controller.

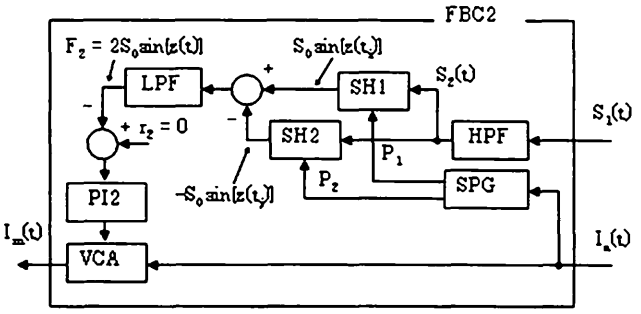

Fig. 3 Block diagram of FBC2: HPF, highpass filter; SPG, sampling pulse generator; SH, sample-and-hold circuits; LPF, lowpass filter; PI2, proportional-integral controller; VCA, voltage-controlled amplifier.

$$I_1(t)=\frac{a^2}{2}\cos 2\omega_c t. \tag{8}$$

Multiplying $S(t)$ and $I_1(t)$ and passing the product through the LPF, as shown in Fig. 2, we can extract the feedback signal[10]

$$F_1(t)=K\cos\alpha(t), \tag{9}$$

from the signal expressed in Eq. (6), where $K=-S_0a^2J_2(Z)/2$. Here PI1 generates the control current $I_c(t)$ so as to realize the condition $F_1(t)=0$. When the control current $I_c(t)$ is injected into the LD, the phase $\alpha(t)$ is automatically adjusted to $\pi/2$. Thus $S(t)$ is converted to

$$S_1(t)=S_{dc1}+S_0\sin(Z\cos\omega_c t). \tag{10}$$

The component S_{dc2} is eliminated completely in Eq. (10). In this process, also the external disturbance is eliminated.

At the same time, we control the modulation amplitude of $S(t)$. Figure 3 shows the block diagram of FBC2 for the MAL control. Because the second term of $S_1(t)$ is the pure ac component, we can easily extract it from $S_1(t)$ by using a HPF as follows:

$$S_2(t)=S_0\sin(Z\cos\omega_c t). \tag{11}$$

The feedback signal for the MAL control is generated from $S_2(t)$ by use of a sampling technique.

Figure 4 illustrates a series of waveforms in the signal processing for the MAL control. The sinusoidal signal $I_a(t)$ [Fig. 4(a)] is fed into the sampling pulse generator (SPG). Then the pulse trains P_1 and P_2 are generated at $t_i=2i\pi/\omega_c$ and $(2j+1)\pi/\omega_c$, respectively, as shown in Figs. 4(b) and 4(c), where i and j are whole numbers. If $S_2(t)$ is alternately sampled and held at t_i and t_j by using sample-and-hold circuits SH1 and SH2, respectively, we obtain signals $g_1(t)=S_0\sin Z$ and $g_2(t)=-S_0\sin Z$ as shown in Fig. 4(d), because $\cos\omega_c t$ becomes ± 1 at t_i and

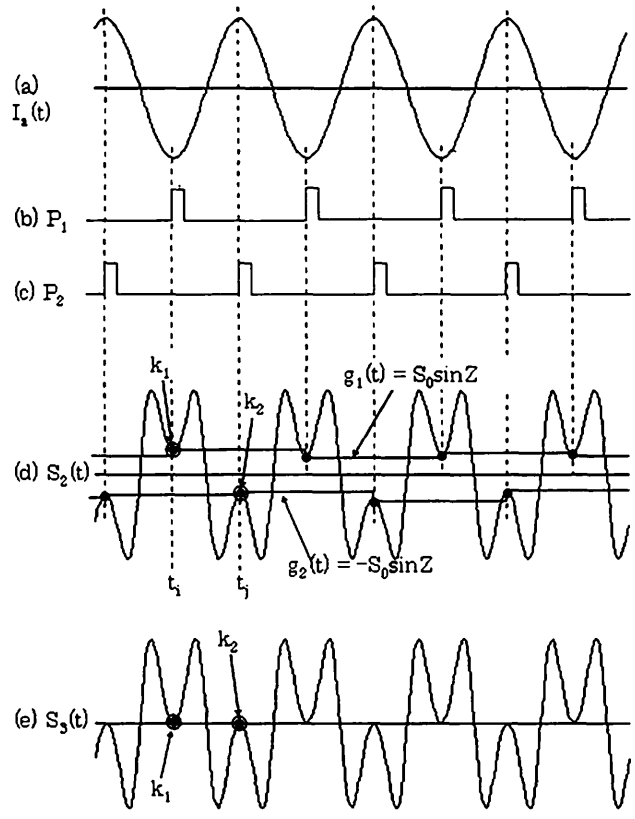

Fig. 4 Schematic of the feedback control: (a) sinusoidal signal for the phase modulation, (b) and (c) sampling pulses, (d) phase-locked signal and generation of the feedback signal, (e) phase-locked and modulation-amplitude-locked signal.

t_j. Subtracting $g_2(t)$ from $g_1(t)$ and passing the difference through a LPF, we obtain the feedback signal

$$F_2(t) = 2S_0 \sin Z. \tag{12}$$

We control $F_2(t)$ to be zero by use of PI controller PI2 as shown in Fig. 3. The amplitude of $I_a(t)$ is properly adjusted with a voltage-controlled amplifier (VCA), and the modulating current $I_m(t)$ locks the modulation amplitude Z at π. If MAL control is achieved, the levels of $g_1(t)$ and $g_2(t)$ coincide with each other. Therefore, we can observe the final signal

$$S_3(t) = S_0 \sin(\pi \cos \omega_c t) \tag{13}$$

as shown in Fig. 4(e), in which both the PL and the MAL control are realized. The phase change from k_1 to k_2 is $2Z = 2\pi$.

The distance L is then expressed as

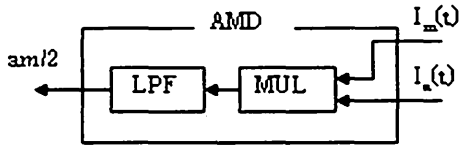

Fig. 5 Block diagram of the amplitude detector: MUL, multiplier; LPF, lowpass filter.

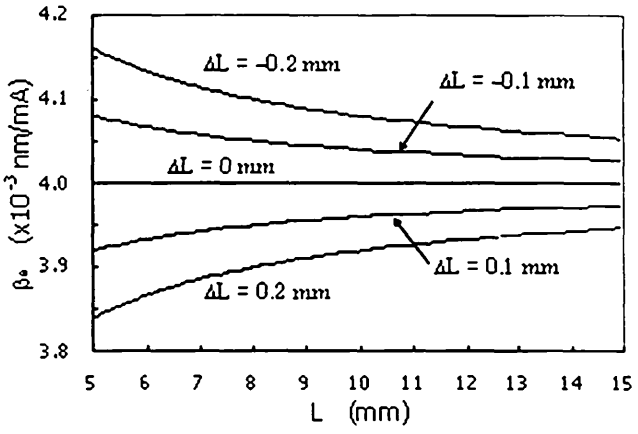

Fig. 6 Dependence of β on OPD error.

$$L = \lambda_0^2 / 4m\beta \tag{14}$$

from Eq. (4). That is, the distance can be measured by detecting the amplitude m of $I_m(t)$. In order to detect m, we evaluate the product

$$I_a(t) \times I_m(t) = \frac{am}{2} + \frac{am}{2} \cos 2\omega_c t. \tag{15}$$

The first term $am/2$ is extracted by use of the LPF, and we can easily detect m because $a/2$ is a constant. The detection of m is implemented in the AMD that is illustrated in Fig. 5.

2.3 *Evaluation of β*

When we determine L with Eq. (14), evaluation of β is important. Substituting π for Z in Eq. (4), β is given by

$$\beta = \lambda_0^2 / 4mL. \tag{16}$$

Equation (16) shows that we can determine β by using the MAL interference signal if L is known exactly. Assuming that L contains an error of ΔL, however, Eq. (16) is expressed as $\beta_e = \lambda_0^2 / 4m(L + \Delta L)$, and it is simply represented by

$$\beta_e = \beta(1 - \Delta L / L) \tag{17}$$

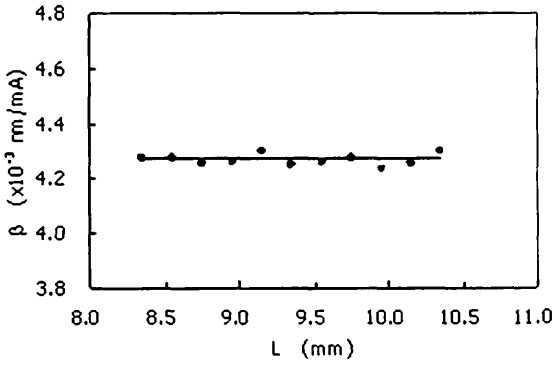

Fig. 7 Measured β versus L.

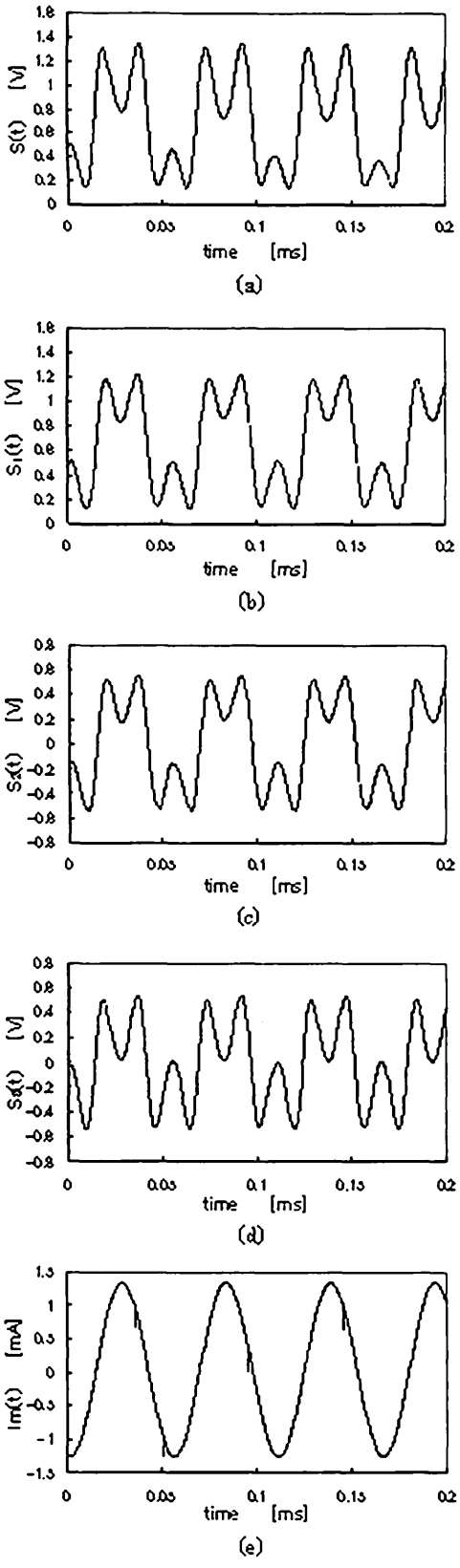

Fig. 8 Observed waveforms in the series in signal processing.

as an approximation. Numerical calculations of β_e are shown in Fig. 6, in which $\lambda_0 = 685.2$ nm, $\beta = 4 \times 10^{-3}$ nm/mA, and the correct m that is obtained when ΔL equals zero were used. We can find some discrepancies

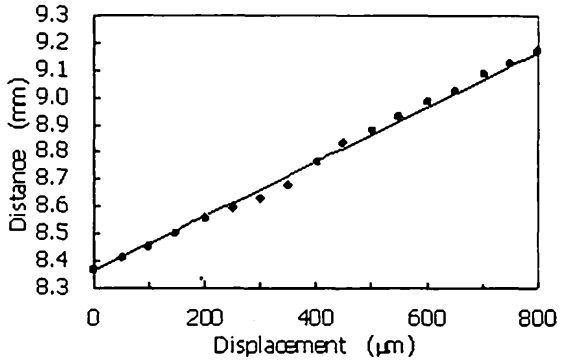

Fig. 9 Absolute distance measured at $L \sim 8$ mm.

between β_e and the exact β when L contains an error, whereas no dependence is observed between β_e and L if they are evaluated exactly.

3 Experiment

The experimental setup is shown in Fig. 1. The initial distance of the Fizeau interferometer was $L_0 \approx 8$ mm. The mirror M is mounted on the x axis stage in a way that allows it to move along the optical axis. The displacement of M is monitored by a dedicated sensor whose resolution is 0.1 μm. The operating wavelength and the maximum output power of the LD are 685.5 nm and 30 mW, respectively. The frequency of the sinusoidal signal $I_a(t)$ was 20 kHz. The cutoff frequencies of the LPF in FBC1, FBC2, and AMD were 4, 2, and 4 kHz, respectively. The cutoff frequency of the HPF in FBC2 was 2 kHz.

First, the modulation efficiency β was evaluated by observing $S(t)$. We moved M from L_0 to $L_0 + 2$ mm in 0.2-mm increments. The value of Z was kept at π by manually adjusting the amplitude of $I_m(t)$ while M was moved. At the same time, the amplitude m was precisely measured. Values of β obtained from Eq. (16) are plotted in Fig. 7. When we set the initial L_0 at 8.36 mm, no dependence was observed between β and L. We can conclude that they are accurately evaluated from the discussion in the previous section. Thus β was determined as 4.27×10^{-3} nm/mA from this experiment.

We next observed waveforms in the series in signal processing as shown in Fig. 8. Here $S(t)$ contains dc components S_{dc1}, S_{dc2} and an external disturbance as shown in Fig. 8(a) when no feedback controls are implemented. When the PL control is applied to $S(t)$, the waveform becomes symmetric as shown in Fig. 8(b). We find that S_{dc2} and the external disturbance are eliminated. Passing $S_1(t)$ through the HPF as shown in Fig. 3, we obtained $S_2(t)$ as shown in Fig. 8(c). This shows that all dc components were removed. Moreover, as illustrated in Fig. 8(d), Z becomes π when the MAL control is achieved. At the same time, the modulating signal $I_m(t)$, which realized the MAL control, was observed as shown in Fig. 8(e). The distance is obtained by use of Eq. (14) after detecting the amplitude of $I_m(t)$.

Finally, the position of the mirror was measured. We moved the mirror from L_0 to $L_0 + 0.8$ mm in 50-μm increments. Measured distances are plotted in Fig. 9 along with

the theoretical solid line whose slope is one. The deviation between the measurements and the theoretical line was estimated as 17.7 μm rms in our prototype. This error will be decreased if the control parameters are appropriately tuned and the wavelength-tuning range is widened by using a wavelength-scanning light source such as a distributed-Bragg-reflector LD.[8,11]

4 Conclusions

A simple range finder that uses an ordinary LD is proposed and demonstrated. Our system requires no complicated phase detection in a computer. The use of both phase-locked and modulation-amplitude-locked controls enables us to realize real-time distance measurements free from external disturbances. Preliminary experiments indicate a measurement error of 17.7 μm rms.

References

1. Y.-Y. Cheng and J. C. Wyant, "Two-wavelength phase shifting interferometry," *Appl. Opt.* **23**(24), 4539–4543 (1984).
2. J. den Boef, "Two-wavelength scanning spot interferometer using single-frequency diode lasers," *Appl. Opt.* **27**(2), 306–311 (1988).
3. C. Williams and H. K. Wickramasinghe, "Optical ranging by wavelength multiplexed interferometry," *J. Appl. Phys.* **60**(6), 1900–1903 (1986).
4. T. Suzuki, T. Muto, O. Sasaki, and T. Maruyama, "Wavelength-multiplexed phase-locked laser diode interferometer using a phase-shifting technique," *Appl. Opt.* **36**(25), 6196–6201 (1997).
5. T. Suzuki, O. Sasaki, and T. Maruyama, "Absolute distance measurement using wavelength-multiplexed phase-locked laser diode interferometry," *Opt. Eng.* **35**(2), 492–497 (1996).
6. T. Suzuki, O. Sasaki, and T. Maruyama, "Phase-locked laser diode interferometry for surface profile measurement," *Appl. Opt.* **28**(20), 4407–4410 (1989).
7. O. Sasaki, T. Yoshida, and T. Suzuki, "Double sinusoidal phase-modulating laser diode interferometer for distance measurement," *Appl. Opt.* **30**(25), 3617–3621 (1991).
8. T. Suzuki, H. Suda, and O. Sasaki, "Double sinusoidal phase-modulating DBR laser diode interferometer for distance measurement," *Appl. Opt.* **42**(1), 60–66 (2003).
9. O. Sasaki, K. Takahashi, and T. Suzuki, "Sinusoidal phase modulating laser diode interferometer with a feedback control system to eliminate external disturbance," *Opt. Eng.* **29**(12), 1511–1515 (1990).
10. T. Suzuki, O. Sasaki, S. Takayama, and O. Sasaki, "Real-time displacement measurement using synchronous detection in a sinusoidal phase modulating laser diode interferometer," *Opt. Eng.* **32**(5), 1033–1037 (1993).
11. G. Mourat, N. Servagent, and T. Bosch, "Distance measurement using the self-mixing effect in a three electrode distributed Bragg reflector laser diode," *Opt. Eng.* **39**(3), 738–743 (2000).

Takamasa Suzuki received his BE degree in electrical engineering from Niigata University in 1982, his ME degree from Tohoku University in 1984, and his PhD degree in electrical engineering from Tokyo Institute of Technology in 1994. He is an associate professor of electrical and electronic engineering at Niigata University. His research interests include optical metrology, optical information processing, and phase-conjugate optics.

Tatsuo Iwana received his BE degree in electrical engineering from Niigata University in 2003. He is currently a master's course student in the Graduate School of Science and Technology at Niigata University. His research interest involves optical metrology. He currently engages in wavelength-scanning interferometry.

Osami Sasaki received his BE and ME degrees in electrical engineering from Niigata University in 1972 and 1974, respectively, and his PhD degree in electrical engineering from Tokyo Institute of Technology in 1981. He is a professor of electrical and electronic engineering at Niigata University. Since 1974, he has worked in the field of optical measuring systems and optical information processing.